chemistry

MDPI

Article

A New Unnatural Amino Acid Derived from the Modification of 4′-(p-tolyl)-2,2′:6′,2″-terpyridine and Its Mixed-Ligand Complexes with Ruthenium: Synthesis, Characterization, and Photophysical Properties

Konstantinos Ypsilantis [1], Antonia Garypidou [1], Andreas Gikas [1], Alexandros Kiapekos [1], John C. Plakatouras [1,2] and Achilleas Garoufis [1,2,*]

[1] Department of Chemistry, University of Ioannina, GR-45110 Ioannina, Greece
[2] Institute of Materials Science and Computing, University Research Centre of Ioannina (URCI), GR-45110 Ioannina, Greece
* Correspondence: agaroufi@uoi.gr

Abstract: The modification of the methyl group of 4′-(p-tolyl)-2,2′:6′,2″-terpyridine produced the novel unnatural amino acid 3-(4-([2,2′:6′,2″-terpyridin]-4′-yl)phenyl)-2-aminopropanoic acid (phet). Mononuclear heteroleptic ruthenium complexes of the general formulae $[Ru(L^1)(L^2)](PF_6)_2$ (L^1 = 2-acetylamino-2-(4-[2,2′:6′,2″]terpyridine-4′-yl-benzyl)-malonic acid diethyl ester, (phem), 3-(4-([2,2′:6′,2″-terpyridin]-4′-yl)phenyl)-2-aminopropanoic acid, (phet), and L^2 = 2,2′:6′,2″-terpyridine (tpy), 4′-phenyl-2,2′:6′,2″-terpyridine (ptpy), 4′-(*p*-tolyl)-2,2′:6′,2″-terpyridine (mptpy)), as well as the homoleptic $[Ru(phem)_2](PF_6)_2$ and $[Ru(phet)_2](PF_6)_2$, were synthesized and characterized by means of NMR spectroscopic techniques, elemental analysis, and high-resolution mass spectrometry. The photophysical properties of the synthesized complexes were also studied.

Keywords: ruthenium; terpyridine; photophysical properties; unnatural amino acid

Citation: Ypsilantis, K.; Garypidou, A.; Gikas, A.; Kiapekos, A.; Plakatouras, J.C.; Garoufis, A. A New Unnatural Amino Acid Derived from the Modification of 4′-(p-tolyl)-2,2′:6′,2″-terpyridine and Its Mixed-Ligand Complexes with Ruthenium: Synthesis, Characterization, and Photophysical Properties. *Chemistry* **2023**, *5*, 151–163. https://doi.org/10.3390/chemistry5010012

Academic Editors: Zoi Lada, Konstantis Konidaris and Guoqi Zhang

Received: 12 December 2022
Revised: 4 January 2023
Accepted: 13 January 2023
Published: 15 January 2023

1. Introduction

Unnatural amino acids (UAAs) are amino acids which are not involved in the protein synthesis process in the cell. They are also called non-proteogenic amino acids. Even though several UAAs frequently occur in nature [1], most of them are chemically synthesized [2,3]. UAAs are promising therapeutic substances as single amino acids [4,5] and scaffolds for peptidomimetics [4,5], precursors in organic synthesis [6], antibody–drug conjugates [7], smart materials [8], and fluorescent probes for biomedical applications [9,10]. Among the various types of UAAs, α-amino acids analogous are very important motifs for pharmaceutical compounds [11–14]. Phenylalanine and tyrosine derivatives are unambiguously the most studied unnatural α-amino acids as they are already in clinical use [15–17]. Several synthetic procedures based on transition metal catalysts to modify the phenylalanine in a highly selective manner have been investigated [18,19].

On the other hand, 2,2′:6′,2″-terpyridines can act as tridentate chelating ligands forming very stable metal complexes. These complexes have attracted research interest due to their unique properties as photoluminescence compounds, DNA binders, sensors, tumour inhibitors and photosensitizers in PDT [20–26]. Despite that, Ru-bis-terpyridine complexes have rarely been investigated as photosensitizers since they do not acquire the appropriate photophysical requirements for PDT [27,28]. However, 4′-substituted terpyridines with proper units may improve the photophysical properties of Ru-bis-terpyridine complexes [29]. Moreover, properly 4′-substituted terpyridines can be used as effective building blocks to form polynuclear metal complexes [30–32]. Thus, Ru-bis-terpyridine mononuclear complexes are linked to each other by various linkers and with various types of bonds [30]

in order to form polymeric structures. The most common types of bonds are: (a) carbon–carbon bonds, as in the cases of phenylene-linked [33] or alkyne-linked complexes [34] and (b) amide bonds that are formed between heteroleptic Ru-bis-terpyridine complexes containing a 4′-carboxyl group-substituted tpy from one side and a 4′-amino group one from the other [35–37]. Additionally, tpy units are incorporated as side chains in polymeric materials producing various interesting structures such as those recently reported by Wang et al. [38]. The synthesized polymer is a novel white-light-emitting fluorescent material. Inspired by the above, we designed and synthesized the UAA 3-(4-([2,2′:6″,2″-terpyridin]-4′-yl)phenyl)-2-aminopropanoic acid (phet) through the modification of 4′-(*p*-tolyl)-2,2′:6′,2″-terpyridine, so it can be potentially used as a building block in the formation of polynuclear metal complexes or polymeric materials (Scheme 1).

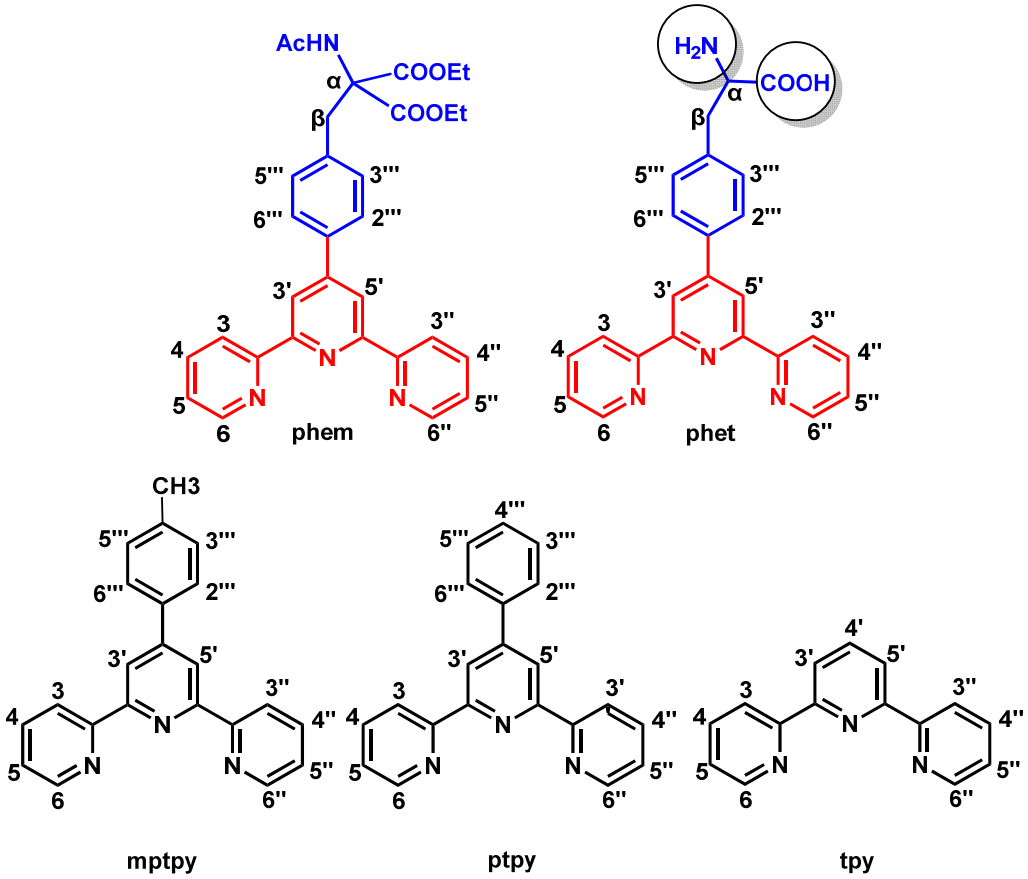

Scheme 1. Structures with numbering of ligands which were involved in this study.

Herein, we also report on the synthesis and characterization of the heteroleptic ruthenium(II) complexes containing phet and its precursor phem, with the general formula $[Ru(L^1)(L^2)](PF_6)_2$ (L^1 = 2-acetylamino-2-(4-[2,2′:6′,2″]terpyridine-4′-yl-benzyl)-malonic acid diethyl ester, (phem), 3-(4-([2,2′:6′,2″-terpyridin]-4′-yl)phenyl)-2-aminopropanoic acid, (phet), and L^2 = 2,2′:6′,2″-terpyridine (tpy), 4′-phenyl-2,2′:6′,2″-terpyridine (ptpy), 4′-(*p*-tolyl)-2,2′:6′,2″-terpyridine (mptpy)), as well as the homoleptic $[Ru(phem)_2](PF_6)_2$ and $[Ru(phet)_2](PF_6)_2$. Additionally, we investigated some photophysical properties of the synthesized complexes.

2. Materials and Methods

2.1. Materials

All solvents were of analytical grade and were used without further purification. 2,2′:6′,2″-terpyridine 98%, 2-acetylpyridine 98%, benzaldehyde 99%, *p*-tolualdehyde 97%, N-bromosuccinimide (NBS) 99%, benzoyl peroxide 70%, and diethyl acetamidomalonate

98% were purchased from Sigma-Aldrich and Alfa Aesar. Hydrated ruthenium trichloride, $RuCl_3 \cdot 3H_2O$, was purchased from Pressure Chemical Company (Pittsburgh, PA, USA). Deuterated solvents for NMR spectroscopy were purchased from Sigma-Aldrich. The compounds 4′-phenyl-2,2′:6′,2″-terpyridine (ptpy) [39], 4′-(4-methylphenyl)-2,2′:6′,2″-terpyridine (mptpy) [40,41], 4′-[4-bromomethyl-phenyl)- 2,2′:6′,2″-terpyridine [40], [Ru(tpy)Cl_3] [42], [Ru(ptpy)Cl_3] [42], and [Ru(mptpy)Cl_3] [42] were synthesized according to the literature methods.

2.2. Methods

C, H, N determinations were performed on a PerkinElmer 2400 series II analyser. Electrospray mass spectra (ESI-MS) were obtained on an Agilent Technology LC/MSD trap SL instrument and Thermo Scientific, LTQ Orbitrap XL™ high-resolution system. Absorption spectra were measured in a Jasco V-650 spectrophotometer in a 1 cm path length cell for the region 900–220 nm. NMR spectra were recorded on Bruker Avance spectrometers operating at proton frequencies of 400.13 and 500.13 MHz and were processed using Topspin 4.07 (Bruker Analytik GmbH, Ettlingen, Germany). Two-dimensional COSY and TOCSY spectra were recorded using the standard Brucker procedures.

2.3. Fluorescence Emission Studies

The fluorescence emission study was carried out using a Jasco FP-8300 fluorometer equipped with a xenon lamp source. The photoluminescence quantum yields of the solutions were calculated by the equation $Q_s = Q_r(A_r/A_s)\,(E_s/E_r)\,(n_s/n_r)^2$, using [Ru(bpy)$_3$]$Cl_2$ in degassed water as a reference standard ($Q_r = 0.04$). 'A' represents the absorbance of the solution, 'E' the integrated fluorescence intensity of the emitted light, 'n' is the refractive index of the solvents and subscripts 'r' and 's' correspond to the reference and the sample, respectively. By the equation $Q = S_2/S_0 - S_1$ the quantum yield of solid state of the complexes were calculated. S_2 denotes the integrated emission intensity of the sample and S_0, S_1 stand for the excitation intensities of the standard and the sample, respectively.

2.4. Synthesis of the Compounds and the Ruthenium Complexes

2-acetylamino-2-(4-[2,2′:6′,2″]terpyridine-4′-yl-benzyl)-malonic acid diethyl ester, (1), (phem): In a single-neck 250 mL round-bottom flask, 100 mL of MeCN, 402 mg (1 mmol) of 4′-[4-bromomethyl-phenyl)-2,2′:6′,2″-terpyridine, 217 mg (1 mmol) of diethyl acetamidomalonate, 276 mg (2 mmol) of K_2CO_3, and 166 mg (1 mmol) of KI were added in this order. The mixture was refluxed for 12 h, cooled at ambient temperature, filtered from the unreacted materials, and the orange solution was evaporated to dryness, under reduced pressure. The crude red-brown solid was dissolved in 100 mL of CH_2Cl_2 and washed three times with 100 mL of distilled water. The organic phase was collected carefully, dried with $MgSO_4$, and evaporated almost to dryness. The microcrystalline pale-yellow product was collected with filtration, washed with toluene, and dried under vacuum over $CaCl_2$. Yield 80% (430 mg). $C_{31}H_{30}N_4O_5$ (538.2): Calc. C, 69.13; H, 5.61; N, 10.40. Found C, 68.82; H, 5.83; N, 10.52. ^{1}H NMR (dmso-d_6, 298 K, δ in ppm, ^{3}J in Hz, 400 MHz) H3H3″ = 8.77 (d, 2H, ^{3}J = 8.0); H4H4″ = 8.05 (t, 2H, ^{3}J = 7.9); H5H5″ = 7.54 (t, 2H, ^{3}J = 7.4); H6H6″ = 8.77 (d, 2H, ^{3}J = 5.3); H2‴H6‴ = 7.87 (d, 2H, ^{3}J = 8.1); H3‴H5‴= 7.20 (d, 2H, ^{3}J = 8.1); H3′H5′ = 8.71 (s, 2H); NH = 8.17 (s, 1H); βCH$_2$- = 3.53 (s, 2H); CH$_3$-[acetylamide] = 2.00 (s, 3H); CH$_3$-[ethylester] = 1.21 (t, 6H, ^{3}J = 6.2); CH$_2$-[ethylester] = 4.20 (q, 4H, ^{3}J = 7.2). HR-ESI-MS: m/z = 539.2280; calculated for $[C_{31}H_{30}N_4O_5 + H]^+$, m/z = 539.2289, assigned to $[(1)H]^+$.

(R, S)-3-(4-([2,2′:6′,2″-terpyridin]-4′-yl)phenyl)-2-aminopropanoic acid (2), (phet): In a single-neck 100 mL round-bottom flask, 50 mL of 6M aqueous HCl and 430 mg (0.8 mmol) of (1) were added. The mixture was refluxed for 48 hours, cooled at ambient temperature, filtered from the impurities, and evaporated to dryness. The solid product was dissolved in 50 mL of distilled water and the pH was adjusted to 4.5–5. After 24 h in the fridge, a microcrystalline solid appeared, and was collected with filtration, washed

two times with 5 mL of H_2O and dried under vacuum over $CaCl_2$. Yield 75% (300 mg). $C_{24}H_{20}N_4O_2$ (396.2): Calc. C, 72.71; H, 5.08; N, 14.13. Found C, 72.52; H, 5.13; N, 14.08. ^{1}H NMR (DCl, pH = 2, 298 K, δ in ppm, ^{3}J in Hz, 400 MHz) H3H3″ = 7.87 (d, 2H, ^{3}J = 8.2); H4H4″ = 8.69 (t, 2H, ^{3}J = 8.2); H5H5″ = 8.08 (t, 2H, ^{3}J = 6.9); H6H6″ = 8.89 (d, 2H, ^{3}J = 6.0); H3′H5′ = 8.71 (s, 2H); H2‴H6‴ = 8.80 (d, 2H, ^{3}J = 8.2); H3‴H5‴ = 7.44 (d, 2H, ^{3}J = 8.2); αCH- = 4.32 (t, 1H, ^{3}J = 6.2); βCH$_2$- = 3.27, 3.30 (m, 2H, $^3J_{H\alpha H\beta 1/H\alpha H\beta 2}$ = 6.3/7.2). HR-ESI-MS: m/z = 397.1644, z = 1; calculated for $[C_{24}H_{20}N_4O_2]^+$, m/z = 397.1659, assigned to [phet]$^+$. ^{1}H NMR (dmso-d$_6$, 298 K, δ in ppm, 400 MHz). [phet]: H3′H5′ = 8.71 (s, 4H); H3H3″ = 8.68 (d, 4H); H4H4″ = 8.04 (t, 4H); H5H5″ = 7.53 (t, 4H); H6H6″ = 8.77 (d, 2H); H2‴H6‴ = 7.86 (d, 4H); H3‴H5‴ = 7.49 (d, 4H); αCH- = 3.44 (m, 1H); βCH$_2$- = 3.30, 3.32 (m, 2H).

Ru(phem)Cl_3, (3): In a solution of 50 mL MeOH containing 130 mg (0.5 mmol) of $RuCl_3 \cdot 3H_2O$, 270 mg (0.5 mmol) of phem was added under continuous stirring. After 1 h at ambient temperature, a dark-red precipitate appeared, which was filtered off, washed two times with 5 mL cold MeOH, and dried under vacuum over $CaCl_2$. Yield 90% (340 mg). $C_{31}H_{30}Cl_3N_4O_5Ru$ (746): Calc. C, 49.91; H, 4.05; N, 7.51. Found C, 49.63; H, 4.22; N, 7.38.

[Ru(tpy)(phem)]$(PF_6)_2$ (4): In a double-neck 100 mL round-bottom flask, 15 mL of ethylene glycol, 45 mg (0.1 mmol) of Ru(tpy)Cl_3, and 54 mg (0.1 mmol) of phem were added. The mixture was heated at reflux under a stream of argon for 12 hours and cooled slowly at ambient temperature, and 20 mL of distilled water was added. To the resulting red solution, about 20 mg (0.1 mmol) of KPF_6 was added under continuous stirring and the mixture was kept overnight in the fridge. The dark-red precipitate was collected through filtration and purified chromatographically as follows: The crude product was dissolved in 2 mL of MeCN:H_2O 6:1, saturated with KNO_3, loaded on a column of silica (30 cm × 2 cm), and eluted with the same solvent. The first red-coloured band was collected and evaporated to dryness. The resulting solid was dissolved in saturated aqueous solution of KPF_6 where the complex (4) was precipitated, collected through filtration, and dried under vacuum over $CaCl_2$. Yield 65% (75 mg). $C_{46}H_{41}F_{12}N_7O_5P_2Ru$ (1162.9): Calc. C, 47.51; H, 3.55; N, 8 [tpy]: H3H3″ = 9.09 (d, 2H, ^{3}J = 8.0); H4H4″ = 8.06 (t, 2H, ^{3}J = 7.8); H5H5″ = 7.28 (t, 2H, ^{3}J = 7.0); H6H6″ = 7.43 (d, 2H, ^{3}J = 5.7); H3′H5′ = 8.84 (d, 2H, ^{3}J = 8.1); H4′ = 8.54 (t, 1H, $^3J_{H3'H4'}$ = 8.1). [phem]: H3H3″ = 9.11 (d, 2H, $^3J_{H3H4}$ = 7.9); H4H4″ = 8.04 (t, 2H, ^{3}J = 7.9); H5H5″ = 7.26 (t, 2H, ^{3}J = 7.5); H6H6″ = 7.51 (d, 2H, ^{3}J = 5.2); H3′H5′ = 9.45 (s, 2H); H2‴H6‴ = 8.38 (d, 2H, ^{3}J = 7.9); H3‴H5‴ = 7.36 (d, 2H, ^{3}J = 7.9); NH = 8.19 (s, 1H); βCH$_2$- = 3.66 (s, 2H); CH$_3$-[acetylamide] = 2.02 (s, 3H); CH$_3$-[ethylester] = 1.23 (t, 6H, ^{3}J = 6.3); CH$_2$-[ethylester] = 4.22(q, 4H, ^{3}J = 7.2). HR-ESI-MS: m/z = 436.6112, z = 2; calculated for $[C_{46}H_{41}N_7O_5Ru]^{2+}$, m/z = 436.6101, assigned to [Ru(tpy)(phem)]$^{2+}$.

[Ru(ptpy)(phem)]$(PF_6)_2$ (5): In a double-neck 100 mL round-bottom flask, 10 mL of ethylene glycol, 53 mg (0.1 mmol) of Ru(ptpy)Cl_3, and 54 mg (0.1 mmol) of phem were added. The mixture was heated at reflux under a stream of argon for 24 h, cooled slowly at ambient temperature, and 20 mL of distilled water was added. To the resulting red solution, about 20 mg (0.1 mmol) of KPF_6 was added under continuous stirring and the mixture was kept overnight in the fridge. The dark-red precipitate was collected through filtration and purified chromatographically as in the case of (1). The resulting solid was dissolved in saturated aqueous solution of KPF_6 where the complex (5) was precipitated, collected by filtration, and dried under vacuum over $CaCl_2$. Yield 65% (82 mg). $C_{52}H_{45}F_{12}N_7O_5P_2Ru$ (1239): Calc. C, 50.41; H, 3.66; N, 7.91. Found C, 50.63; H, 3.82; N, 7.96. ^{1}H NMR (dmso-d$_6$, 298 K, δ in ppm, ^{3}J in Hz, 400 MHz). [ptpy]: H3H3″ = 9.11 (d, 2H, ^{3}J = 8.2); H4H4″ = 8.06 (t, 2H, ^{3}J = 8.2); H5H5″ = 7.28 (t, 2H, ^{3}J = 8.0); H6H6″ = 7.53 (d, 2H, ^{3}J = 5.5); H3′H5′ = 9.46 (s, 2H); H2‴H6‴ = 8.44 (d, 2H, ^{3}J = 7.9); H3‴H5‴ = 7.77 (t, 2H, ^{3}J = 7.9); H4‴ = 7.69 (t, 1H, ^{3}J = 7.1); [phem]: H3H3″ = 9.11 (d, 2H, ^{3}J = 8.2); H4H4″ = 8.06 (t, 2H, ^{3}J = 8.1); H5H5″ = 7.27 (t, 2H, ^{3}J = 8.0); H6H6″ = 7.53 (d, 2H, ^{3}J = 5.5); H3′H5′ = 9.47 (s, 2H); H2‴H6‴ = 8.44 (d, 2H, ^{3}J = 7.9); H3‴H5‴ = 7.37 (d, 2H, ^{3}J = 7.9); NH = 8.19 (s, 1H); βCH$_2$- = 3.66 (s, 2H); CH$_3$-[acetylamide] = 2.04 (s, 3H); CH$_3$[ethylester] = 1.25 (t, 6H,

^{3}J = 6.3); CH_2[ethylester] = 4.22 (q, 4H, ^{3}J = 7.2). HR-ESI-MS: m/z = 474.6272, z = 2; calculated for $[C_{52}H_{45}N_7O_5Ru]^{2+}$, m/z = 474.6257, assigned to $[Ru(ptpy)(phem)]^{2+}$.

[Ru(mptpy)(phem)]$(PF_6)_2$ (6): In a double-neck 100 mL round-bottom flask, 10 mL of ethylene glycol, 55 mg (0.1 mmol) of Ru(mptpy)Cl_3, and 54 mg (0.1 mmol) phem were added. The mixture was heated at reflux under a stream of argon for 24 h, cooled slowly at ambient temperature, and 10 mL of distilled water were added. To the resulting red solution, about 20 mg (0.1 mmol) of KPF_6 was added under continuous stirring and the mixture was kept overnight in the fridge. The dark-red precipitate was collected through filtration and purified chromatographically as in the case of (1). The resulting solid was dissolved in saturated aqueous solution of KPF_6 where the complex (6) was precipitated, collected by filtration and dried under vacuum over $CaCl_2$. Yield 70% (89 mg). $C_{53}H_{47}F_{12}N_7O_5P_2Ru$ (1253): Calc. C, 50.80; H, 3.78; N, 7.83. Found C, 50.68; H, 3.85; N, 7.68. ^{1}H NMR (dmso-d_6, 298 K, δ in ppm, ^{3}J in Hz, 400 MHz) [mptpy]: H3′H5′ = 9.47 (s, 2H); H3H3″ = 9.11 (d, 2H, ^{3}J = 8.0); H4H4″ = 8.07 (t, 2H, ^{3}J = 7.8); H5H5″ = 7.27 (t, 2H, ^{3}J = 7.9); H6H6″ = 7.54 (d, 2H, ^{3}J = 5.5); H2‴H6‴ = 8.38 (d, 2H, ^{3}J = 7.9); H3‴H5‴ = 7.58 (d, 2H, ^{3}J = 7.9); βCH_3 = 3.05 (s, 3H). [phem]: H3H3″ = 9.11 (d, 2H, ^{3}J = 8.0); H4H4″ = 8.07 (t, 2H, ^{3}J = 8.0); H5H5″ = 7.27 (d, 2H, ^{3}J = 7.9); H6H6″ = 7.54 (d, 2H, ^{3}J = 5.5); H3′H5′ = 9.47 (s, 2H); H2‴H6‴ = 8.42 (d, 2H, ^{3}J = 8.5); H3‴H5‴ = 7.37 (d, 2H, ^{3}J = 8.5); NH = 8.18 (s, 1H); βCH_2- = 3.67 (s, 2H); CH_3-[acetylamide] = 2.05 (s, 3H); CH_3-[ethylester] = 1.26 (t, 6H, ^{3}J = 6.3); CH_2-[ethylester] = 4.23 (q, 4H, ^{3}J = 7.2). HR-ESI-MS: m/z = 481.6337, z = 2; calculated for $[C_{53}H_{47}N_7O_5Ru]^{2+}$, m/z = 481.6336, assigned to $[Ru(mptpy)(phem)]^{2+}$.

[Ru(phem)$_2$]$(PF_6)_2$ (7): In a double-neck 100 mL round-bottom flask, 15 mL of ethylene glycol, 76 mg (0.1 mmol) of Ru(phem)Cl_3, and 54 mg (0.1 mmol) phem were added. The mixture was heated at reflux under a stream of argon for 24 hours, cooled slowly at ambient temperature, and 20 mL of distilled water was added. To the resulting red solution, about 20 mg (0.1 mmol) of KPF_6 was added and the mixture was kept overnight in the fridge. The red precipitate was collected through filtration and purified chromatographically as in the case of complex (1). The resulting solid was dissolved in saturated aqueous solution of KPF_6 where the complex (7) was precipitated, collected by filtration, and dried under vacuum over $CaCl_2$. Yield 50% (73 mg). $C_{62}H_{60}F_{12}N_8O_{10}P_2Ru$ (1468.2): Calc. C, 50.72; H, 4.12; N, 7.63. Found C, 50.41; H, 4.23; N, 7.68. ^{1}H NMR (dmso-d_6, 298 K, δ in ppm, ^{3}J in Hz, 400 MHz). [phem]: H3H3″ = 9.12 (d, 2H, ^{3}J = 8.0); H4H4″ = 8.06 (t, 2H, ^{3}J = 8.0); H5H5″ = 7.27 (t, 2H, ^{3}J = 7.5); H6H6″ = 7.52 (d, 2H, ^{3}J = 6.0); H3′H5′ = 9.47 (s, 2H); H2‴H6‴ = 8.39 (d, 2H, ^{3}J = 8.2); H3‴H5‴ = 7.36 (d, 2H, ^{3}J = 8.2); NH = 8.22 (s, 1H); βCH2- = 3.65(s, 2H); CH3-[acetylamide] = 2.04 (s, 3H); CH_3[ethylester] = 1.24 (t, 6H, ^{3}J = 6.3); CH_2 [ethylester] = 4.23(q, 4H, ^{3}J = 7.2). HR-ESI-MS: m/z = 589.1754, z = 2; calculated for $[C_{62}H_{60}N_8O_{10}Ru]^{2+}$, m/z = 589.1732, assigned to $[Ru(phem)_2]^{2+}$.

The complexes, [Ru(tpy)(phet)]$(PF_6)_2$ (8), [Ru(ptpy)(phet)]$(PF_6)_2$ (9), [Ru(mptpy)(phet)] $(PF_6)_2$ (10) and [Ru(phet)$_2$]$(PF_6)_2$ (11) were prepared similarly. In a typical experiment, 50 mg of the corresponding parent complex (4)–(7) was transferred in a single-neck 100 mL round-bottom flask and 10 mL of aqueous 3M HCl was added. The suspension was heated at reflux for 72 h under N_2 and evaporated to dryness under reduced pressure. The red solid was then dissolved in 50 mL of distillate water and 50 mg of KPF_6 was added under continuous stirring. A dark-red microcrystalline product appeared after cooling the solution overnight in the fridge, was washed several times with cold H_2O, and was dried under vacuum over $CaCl_2$. The yield ranged from 75 to 85% depending on the complex.

[Ru(tpy)(phet)]$(PF_6)_2$ (8): Yield 80%. $C_{39}H_{31}F_{12}N_7O_2P_2Ru$ (1020.7): Calc. C, 45.89; H, 3.06; N, 9.61. Found C, 46.12; H, 3.23; N, 9.52. ^{1}H NMR (dmso-d_6, 298 K, δ in ppm, ^{3}J in Hz, 400 MHz). [tpy]: H4′ = 8.53 (t, 1H, ^{3}J = 8.1); H3′H5′ = 8.85 (d, 2H, ^{3}J = 8.1); H3H3″ = 9.15 (d, 2H, ^{3}J = 8.2); H4H4″ = 8.03 (t, 2H, ^{3}J = 8.2); H5H5″ = 7.27 (t, 2H, ^{3}J = 7.9); H6H6″ = 7.52 (d, 2H, ^{3}J = 5.0). [phet]: H3H3″ = 9.11 (d, 2H, ^{3}J = 7.9); H4H4″ = 8.05 (t, 2H, ^{3}J = 8.2); H5H5″ = 7.28 (t, 2H, ^{3}J = 7.9); H6H6″ = 7.52 (d, 2H, ^{3}J = 5.0); H3′H5′ = 9.49 (s, 2H); H2‴H6‴ = 8.46 (d, 2H, ^{3}J = 8.1); H3‴H5‴ = 7.68 (d, 2H, ^{3}J = 8.1); αCH = 3.68 (t, 1H, $^3J_{H\alpha H\beta}$

= 6.1); βCH$_2$ = 3.32, 3.38 (m, 2H, $^3J_{H\alpha H\beta 1/H\alpha H\beta 2}$ = 6.1/7.3). HR-ESI-MS: m/z = 365.5789, z = 2; calculated for $[C_{39}H_{31}N_7O_2Ru]^{2+}$, m/z = 365.5786, assigned to $[Ru(tpy)(phet)]^{2+}$.

[Ru(ptpy)(phet)](PF$_6$)$_2$ (9): Yield 75%. $C_{45}H_{35}F_{12}N_7O_2P_2Ru$ (1096.8): Calc. C, 49.28; H, 3.22; N, 8.94. Found C, 49.72; H, 3.39; N, 8.79. ^{1}H NMR (dmso-d$_6$, 298 K, δ in ppm, ^{3}J in Hz, 400 MHz). [ptpy]: H3′H5′ = 9.48 (s, 2H); H3H3″ = 9.12 (d, 2H, ^{3}J = 8.1); H4H4″ = 8.08 (t, 2H, ^{3}J = 8.0); H5H5″ = 7.27 (t, 2H, ^{3}J = 7.6); H6H6″ = 7.53 (d, 2H, ^{3}J = 5.1); H2‴H6‴ = 8.43 (d, 2H, ^{3}J = 8.0); H3‴H5‴ = 7.77 (t, 2H, ^{3}J = 8.0); H4‴ = 7.68 (t, 1H, ^{3}J = 7.6); [phet]: H3′H5′ = 9.48 (s, 2H); H3H3″ = 9.12 (d, 2H, ^{3}J = 8.2); H4H4″ = 8.08 (t, 2H, ^{3}J = 8.2); H5H5″ = 7.28 (t, 2H, ^{3}J = 7.9); H6H6″ = 7.53 (d, 2H, ^{3}J = 5.1); H2‴H6‴ = 8.45 (d, 2H, ^{3}J = 8.0); H3‴H5‴ = 7.66 (d, 2H, ^{3}J = 8.0); αCH = 3.60 (t, 1H, ^{3}J = 6.0); βCH$_2$ = 3.32, 3.38 (m, 2H, $^3J_{H\alpha H\beta 1/H\alpha H\beta 2}$ = 6.1/7.2). HR-ESI-MS: m/z = 403.5938, z = 2; calculated for $[C_{45}H_{35}N_7O_2Ru]^{2+}$, m/z = 403.5942, assigned to $[Ru(ptpy)(phet)]^{2+}$.

[Ru(mptpy)(phet)](PF$_6$)$_2$ (10): Yield 80%. $C_{46}H_{37}F_{12}N_7O_2P_2Ru$ (1110.8): Calc. C, 49.74; H, 3.36; N, 8.83. Found C, 50.02; H, 3.44; N, 8.72. ^{1}H NMR (dmso-d$_6$, 298 K, δ in ppm, ^{3}J in Hz, 400 MHz). [mptpy]: H3′H5′ = 9.48 (s, 2H); H3H3″ = 9.11(d, 2H, ^{3}J = 8.1); H4H4″ = 8.06 (t, 2H, ^{3}J = 8.0); H5H5″ = 7.27 (t, 2H, ^{3}J = 7.6); H6H6″= 7.56 (d, 2H, ^{3}J = 5.0); H2‴H6‴ = 8.38, (d, 2H, ^{3}J = 8.0); H3‴H5‴ = 7.58 (d, 2H, ^{3}J = 8.0); phCH$_3$ = 3.05 (s, 3H). [phet]: H3′H5′ = 9.46 (s, 2H); H3H3″ = 9.11(d, 2H, ^{3}J = 8.0); H4H4″ = 8.07 (t, 2H, ^{3}J = 8.0); H5H5″ = 7.28 (t, 2H, ^{3}J = 7.9); H6H6″ = 7.56(d, 2H, ^{3}J = 5.0); H2‴H6‴ = 8.45 (d, 2H, ^{3}J = 8.0); H3‴H5‴ = 7.66 (d, 2H, ^{3}J = 8.0); αCH = 3.57 (t, 1H, ^{3}J = 6.0); βCH$_2$ = 3.29, 3.37 (m, 2H, $^3J_{H\alpha H\beta 1/H\alpha H\beta 2}$ = 6.0/7.0). HR-ESI-MS: m/z = 410.6013, z = 2; calculated for $[C_{46}H_{37}N_7O_2Ru]^{2+}$, m/z = 410.6021, assigned to $[Ru(mptpy)(phet)]^{2+}$.

[Ru(phet)$_2$](PF$_6$)$_2$ (11): Yield 85%. $C_{48}H_{40}F_{12}N_8O_4P_2Ru$ (1183.9): Calc. C, 48.70; H, 3.41; N, 9.46. Found C, 49.01; H, 3.50; N, 9.42. ^{1}H NMR (dmso-d$_6$, 298 K, δ in ppm, 400 MHz). [phet]: H3′H5′ = 9.47 (s, 4H); H3H3″ = 9.12 (d, 4H, ^{3}J = 8.2); H4H4″ = 8.07 (t, 4H, ^{3}J = 7.5); H5H5″ = 7.28 (t, 4H, ^{3}J = 7.5); H6H6″ = 7.53 (d, 2H, ^{3}J = 5.6); H2‴H6‴ = 8.40 (d, 4H, ^{3}J = 7.8); H3‴H5‴ = 7.66 (d, 4H, ^{3}J = 7.8); αCH- = 3.62 (t, 2H, ^{3}J = 5.4); βCH$_2$- = 3.29, 3.38 (m, 4H, $^3J_{H\alpha H\beta 1/H\alpha H\beta 2}$ = 4.2/6.5). ESI-MS: m/z = 447.1119, z = 2; calculated for $[C_{48}H_{40}N_8O_4Ru]^{2+}$, m/z = 447.1103, assigned to $[Ru(phet)]^{2+}$.

3. Results and Discussion

3.1. Synthesis

The ligand phet was synthesized through the following steps: (i) the selective bromination of the -CH$_3$ group of mptpy with N-bromosuccinimide (NBS) in CCl$_4$ using benzoyl peroxide as a radical initiator, (ii) the addition of the diethyl acetamidomalonate anion on the bromo-derivative and isolation of phem (**1**) and (iii) the acidic hydrolysis of the amide, ester, and decarboxylation of (**1**) forming the hydrochloric salt phet·HCl. Adjusting the pH between 4.5 and 5, the pure amino acid phet (**2**) precipitated. The synthetic procedure is summarized in Scheme 2.

With the aim to isolate the complexes of the general formula [Ru(L^1)(phet)](PF$_6$)$_2$ (L^1 = tpy, ptpy, mptpy), we initially synthesized the complexes [Ru(L^1)(phem)]$^{2+}$. The reason is that, in contrast to phem, the ligand phet possesses an active carboxyl and amino group, which may potentially coordinate with the ruthenium centre. Attempts to synthesize these complexes through the reaction between the ligand phet and the corresponding complexes Ru(tpy)Cl$_3$, Ru(mtpy)Cl$_3$, Ru(phem)Cl$_3$ and Ru(phet)Cl$_3$ were made; however, mixtures of several products were observed. Thus, initially, we prepared the complexes (**4**)–(**7**) through the reaction of phem with their corresponding complexes in ethylene glycol and isolated them as $[PF_6]^-$ salts. From boiling ethylene glycol, the Ru(III) was reduced to Ru(II) while oxidation species such as glyoxal and glycolaldehyde were formed. The isolated complexes (**4**)–(**7**) were subjected to acetic hydrolysis of the amide and diethyl esters, as well as decarboxylation of the phem Cα, forming the complexes (**8**)–(**11**) (Scheme 3).

3.2. Characterization

The ^{1}H NMR spectrum of phem in dmso-d_6 (Figure 1) showed significant differences from the spectrum of the original compound mptpy. Specifically, a new signal at 8.17 ppm was assigned to the NH amide proton, while the new signals in the aliphatic part of the spectrum were assigned to the acetyl group (CH_3-acetylamide 2.00 ppm) and the methyl (1.21 ppm) or ethyl (4.20 ppm) groups of malonate ethyl esters. In addition, a singlet at 3.53 ppm was assigned to the protons of the βCH_2. The aromatic protons of the phenyl-terpyridine moiety of phem shifted marginally in the range of $\pm$ 0.05 ppm, compared to the mptpy. However, the H3‴H5‴ shifted downfield by 0.25 ppm, indicating that the modification in the Cβ affects the neighbouring protons.

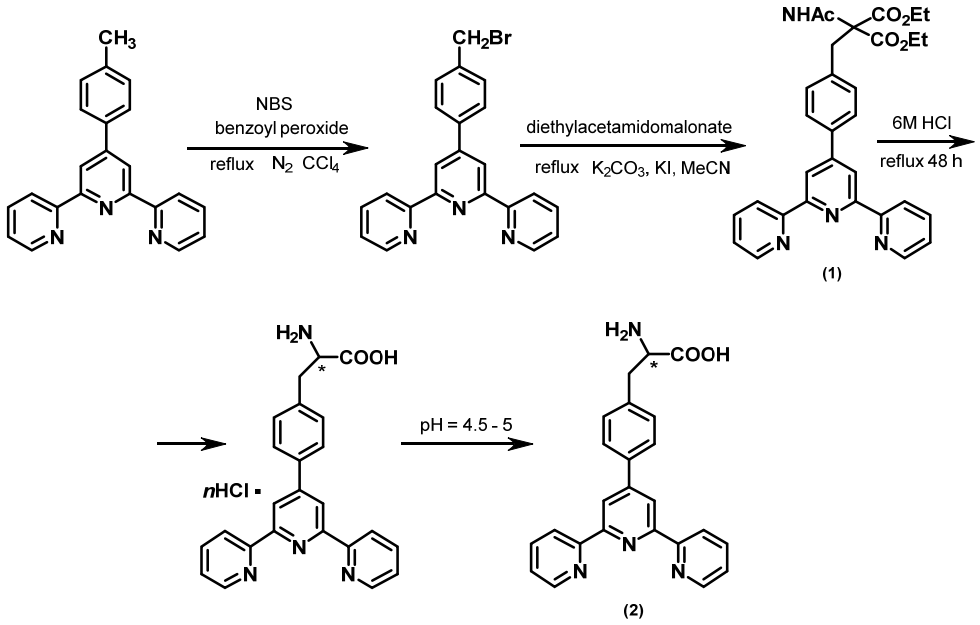

Scheme 2. Reactions and conditions of the synthetic procedure of phet.

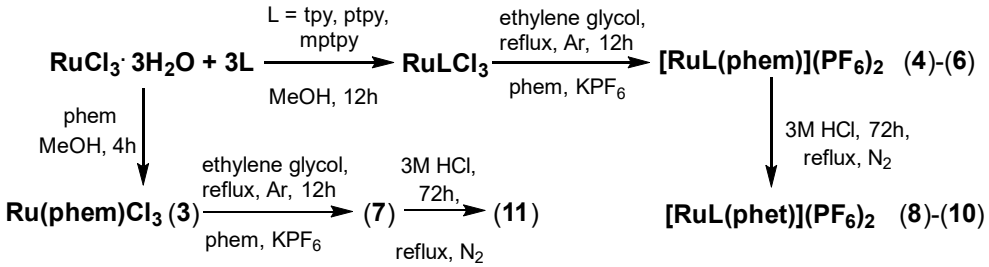

Scheme 3. The formation of the ruthenium complexes (**3**)–(**11**).

After the hydrolysis and decarboxylation of phem, the unnatural amino acid phet was formed. The proton signals of the acetamide NH and -CH_3, as well as the signals of the malonate ethyl esters, were absent, indicating that the hydrolysis of these groups was achieved. In addition, a signal at 4.61 ppm was assigned to αCH, while the signals at 2.94 and 2.96 were assigned to the non-equivalent protons βCHA and βCHB. Additionally, the neighboring phenyl group protons H3‴H5‴ shifted further downfield from phem by 0.29 ppm. Phet is very soluble in DCl (0.01 M) which is an appropriate solvent for further NMR studies. At this pH, phet is protonated in the pyridine rings of tpy and the amino group of αC. In the aliphatic part of the spectrum, only two signals appeared assignable to αCH (4.32) and βCH_A and H_B (3.25 and 3.29 ppm). Once again, the two protons of βC, HA and HB are chemically non-equivalent and coupled further with the H_X of αC, forming an ABX spin-splitting pattern (Figure 2a).

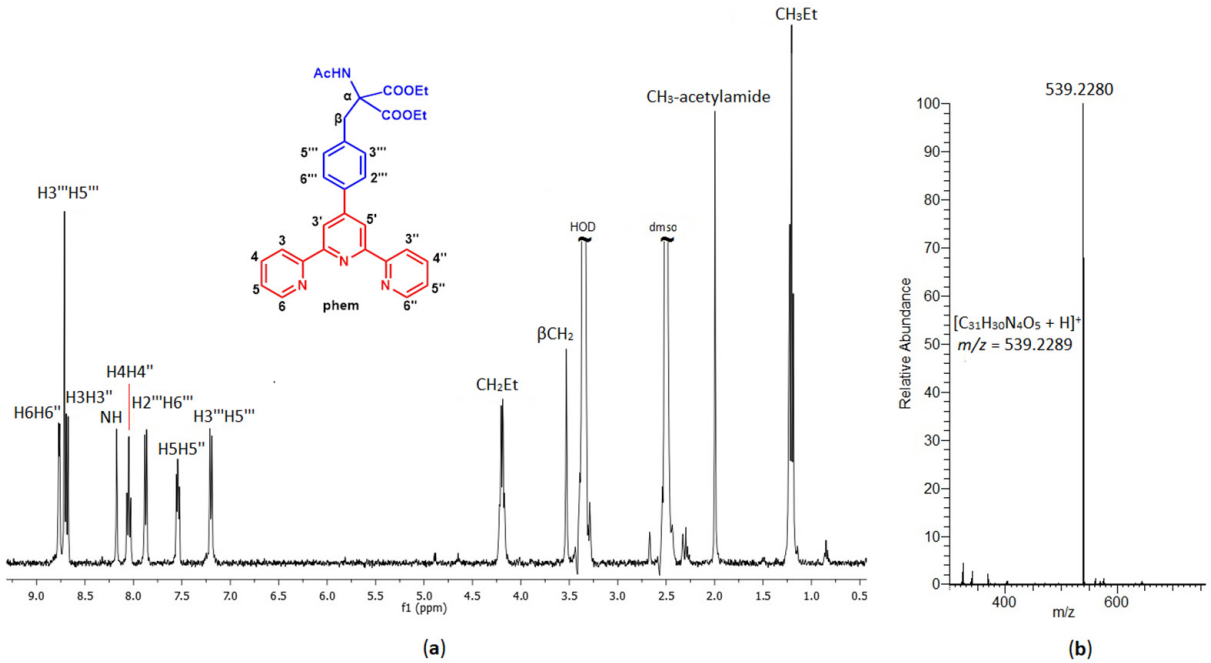

Figure 1. (**a**) The ^{1}H NMR spectrum (dmso-d$_6$, 298 K, δ ppm) of phem with structure numbering and proton assignments. (**b**) The HR-ESI-MS of phem.

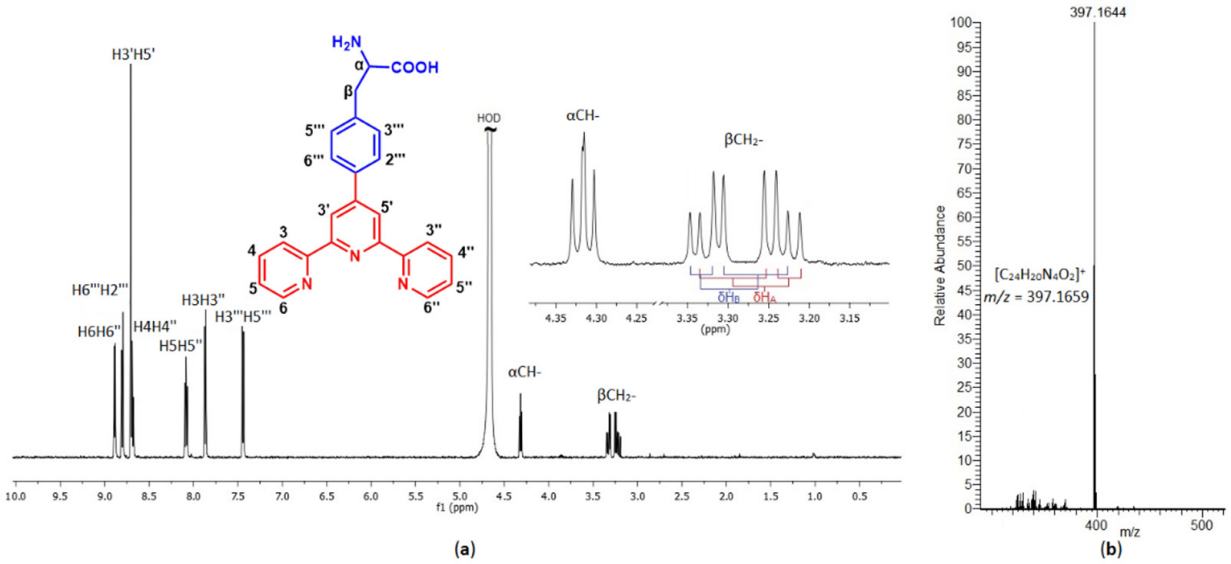

Figure 2. (**a**) The ^{1}H NMR spectrum (DCl 0.01 M, 298 K, δ ppm) of phet with structure numbering and proton assignments. Inset, expansion of the aliphatic part of the spectrum showing the ABX proton spin system between αC and βC. (**b**) The HRESIMS of phem.

Complex (**3**) is insoluble in most of the common organic solvents. In order to form the homoleptic complex $[Ru(phem)_2]^{2+}$, it was used without further characterization. In the aromatic part of the ^{1}H NMR spectrum of (**4**), the signals of the ending pyridine rings of tpy and phem overlapped, apart from those of terpyridines H6H6″ and phemH6H6″ which, in the cases of (**4**) (7.52, 7.43 ppm) and (**8**) (7.68, 7.52 ppm), appeared separately (Figure S1). These signals shifted upfield by 1.22 and 1.34 ppm, respectively, despite being expected to shift downfield, due to the coordination of the neighboring nitrogen atoms to the ruthenium center. This effect was observed for all the complexes (**4**)–(**11**) and was attributed to the perpendicular orientation of H6H6″ towards the metal t2g electron density and the π electron cloud of the other terpyridine ligands (phem or tpy) [43,44]. On the

other hand, the signals of the middle pyridine protons, H3′H5′ and phem H3′H5′or phet H3′H5′, shifted significantly downfield, as expected (e.g., for (**4**) tpy H3′H5′ = 0.39 and phem H3′H5′ = 0.74 ppm).

In the aliphatic part of the ^{1}H NMR spectra of (**8**)–(**11**) (Figures S5–S11) only the proton signals of αCH and βCH$_2$ appeared, as well as the methyl group in the case of (**10**). Compared to the free phet in dmso-d$_6$, the signals of βCH shifted slightly downfield probably indicating a conformational change in the Cβ-Ca bonds, due to the coordination of the terpyridine moiety of phet to the ruthenium center. However, the αCH shifted downfield by 0.13–0.24 ppm depending on the nature of the coordinated terpyridine.

3.3. Photophysical Studies

The absorption spectra of the complexes (**4**)–(**7**) and (**8**)–(**11**) are presented in Figure 3, while their photophysical data are summarized in Table 1. In general, the spectra of (**4**)–(**7**) and (**8**)–(**11**) are similar to each other, displaying a typical spectrum of Ru(II)-bis-terpyridine complex [45]. In the UV spectrum of (**1**), two absorption bands were observed at 251 and 277 nm, assigned to $\pi \rightarrow \pi^*$ intra-ligand transitions as expected [33,46]. Similarly, in the spectrum of (**2**), the initial bands were slightly shifted due to the hydrolysis of the malonate ester and the decarboxylation of Cα. In the cases of (**4**)–(**7**) and (**8**)–(**11**), these bands shifted at lower energy, ranging from 286 to 289 nm and from 305 to 313 nm, respectively, depending on the nature of the additionally coordinated terpyridine. Additionally, hyperchromic or hypochromic effects were observed, due to the different contribution of each ligand to the $\pi \rightarrow \pi^*$ transition.

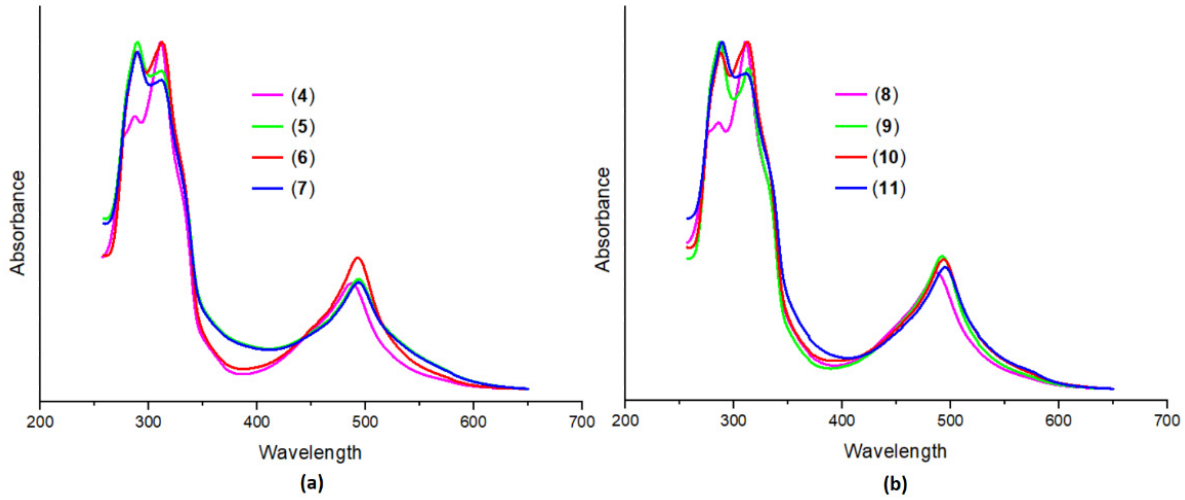

Figure 3. Normalized UV-Vis spectra of the complexes (**a**), (**4**)–(**7**) and (**b**), (**8**)–(**11**) in acetonitrile.

Table 1. Photophysical data for (**1**), (**2**) and (**4**)–(**11**) in solid state and in acetonitrile solution.

	Absorption [298 K]	**Excitation 298 K**		**Emission 298 K**			
	λ_{max} [nm], ($\varepsilon \times 10^3$ M^{-1}cm^{-1})	**Solid λ_{exc} [nm]**	**Solution λ_{exc} [nm]**	**Solid λ_{em} [nm]**	**Q (%)**	**Solution λ_{em} [nm]**	**Q (%)**
(**1**)	251 (23.5), 277 (28.0), 306 sh	-	-	-	-	-	-
(**4**)	286 (33.7), 308 (46.5), 487 (15.5)	-	-	-	-	-	-
(**5**)	284 (56.8), 310 (54.0), 489 (19.7)	-	-	-	-	-	-
(**6**)	286 (50.8), 311 (51.6), 489 (19.8)	-	-	-	-	-	-
(**7**)	286 (51.2), 309 (53.2), 493 (20.5)	-	-	-	-	-	-
(**2**)	252 (19.6), 281 (23.0), 311 sh	350	280	404, 505	0.75	355	0.97
(**8**)	286 (30.0), 311 (39.3), 488 (15.1)	466	488	502, 521, 575	1.20	637	0.95
(**9**)	287 (28.4), 313 (36.3), 490 (15.1)	466	488	503, 520, 575	0.22	646	0.11
(**10**)	289 (33.9), 310 (36.0), 489 (14.2)	470	494	501, 521, 574	0.87	648	0.76
(**11**)	288 (21.6), 305 (20.2), 491 (9.2)	470	493	500, 522, 575	3.32	645	1.81

The absorption bands which were observed between 488 and 491 nm were assigned to metal-to-ligand-charge-transfer (MLCT) with molar coefficients (ε) varying from 9.2 to 14.2 $\times$ 10^3 $M^{-1}cm^{-1}$. In general, our results are consistent with the previous report of Maestri et al. that the substitution in the 4′ position of the terpyridine with electron donating or accepting groups significantly affects the maxima of their MLCT band [47]. Comparing the MLCT λ_{max} of the homoleptic (**7**) and (**11**) with that of the similar $[Ru(tpy)_2](PF_6)_2$ and $Ru(ptpy)_2](PF_6)_2$ in acetonitrile, a gradient red shift of the MLCT maxima was observed. The low energy shift can be corelated to the electron donation of the tpy 4′-substituents following the order: $[Ru(tpy)_2](PF_6)_2$, 474 nm < $[Ru(ptpy)_2](PF_6)_2$, 488 nm < $[Ru(phet)_2](PF_6)_2$, 491 nm < $[Ru(phem)_2](PF_6)_2$, 493 nm.

The emission and excitation data of the synthesized complexes and the free ligands in degassed acetonitrile solution and in solid state are presented in Table 1. By exciting the ligands (**1**) and (**2**) in the solid state, with λ_{exc} 311 and 350 nm, respectively, a weak green emission at 550 nm with low photoluminescent quantum yield was observed only for (**2**), while (**1**) was practically non-emitting.

Upon the excitation of complexes (**4**)–(**7**), both in acetonitrile solution and in the solid state, practically no emission was observed. On the other hand, the complexes (**8**)–(**11**) in acetonitrile emitted similarly at about 637–648 nm with low quantum yields which were calculated at about 1 to 2% (Figure 4). This is expected for Ru(II) complexes with 4′-substituted terpyridines [46]. Similar results have been reported previously by Zhang et al. [48] where Ru(II) complexes with 4,4′ substituted 2,2′-bipyridine were applied as sensitive luminescence probes for detection of cysteine (Cys) and homocysteine (Hcy). The reaction of the non-luminescent probe with Cys and Hcy was accompanied by a notable luminescence increase. In the solid state, the complexes had similar spectra, producing a green emission with low quantum yields in the range of 0.1 to 3% depending on the nature of the coordinated ligands. Complex (**11**) was the most emissive (Q~3.3%) while (**9**) marginally emitted. All spectra showed a vibronic structure with vibronic spacing about 1750 and 800 cm^{-1} due to the high energy vibrations of the ligands. In general, emission was derived from the triplet excited states, mixed with ^{3}MLCT and ^{3}IL [49,50].

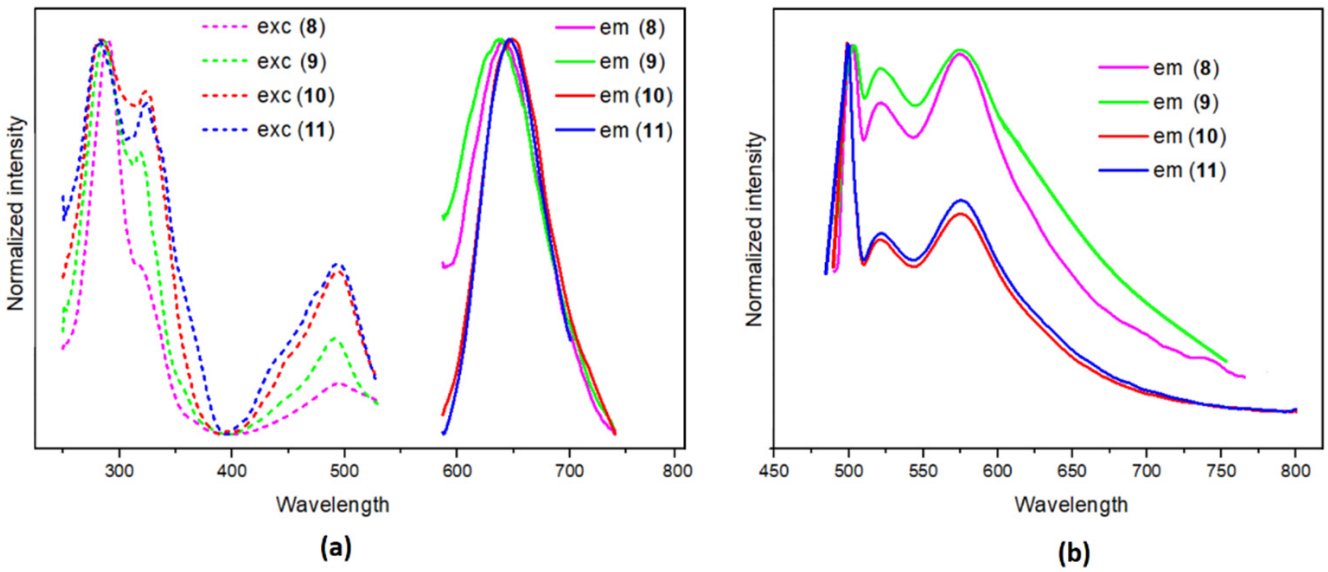

Figure 4. (**a**) Intensity-normalized emission and excitation spectra of (**8**)–(**11**) in acetonitrile at 298 K. (**b**) Intensity-normalized solid state emission spectra of (**8**)–(**11**) at 298 K.

4. Conclusions

The synthesis of the novel UAA 3-(4-([2,2′:6′,2″-terpyridine]-4′-yl)phenyl)-2-aminopropanoic acid (phet) through the modification of 4′-(*p*-tolyl)-2,2′:6′,2″-terpyridine was achieved. Mononuclear heteroleptic ruthenium complexes of the general formulae

$[Ru(L^1)(L^2)](PF_6)_2$, as well as the homoleptic $[Ru(phem)_2](PF_6)_2$ and $[Ru(phet)_2](PF_6)_2$, were synthesized and characterized. These complexes can be potentially used as a building block in the formation of polynuclear ruthenium complexes linked through amide bonds of the phet amino and carboxyl group. The photophysical properties of the synthesized complexes show that the complexes (**8**)–(**11**) emit moderately, while the homoleptic (**11**) is the most emissive in the solid state and acetonitrile solution, with a photoluminescent quantum yield of 2–3%.

Supplementary Materials: The following supporting information can be downloaded at: https://www.mdpi.com/article/10.3390/chemistry5010012/s1, Figure S1: ^{1}H NMR spectrum of (4) with proton assignments in dmso-d_6 at 298 K. Figure S2: ^{1}H NMR spectrum of (5) with proton assignments in dmso-d_6 at 298 K. Figure S3: ^{1}H NMR spectrum of (6) with proton assignments in dmso-d_6 at 298 K. FIGURE S4: ^{1}H NMR spectrum of (7) with proton assignments in dmso-d_6 at 298 K. Figure S5: ^{1}H NMR spectrum of (8) with proton assignments in dmso-d_6 at 298 K. Figure S6: ^{1}H NMR spectrum of (9) with proton assignments in dmso-d_6 at 298 K. Figure S7: ^{1}H NMR spectrum of (10) with proton assignments in dmso-d_6 at 298 K. FIGURE S8: ^{1}H NMR spectrum of (11) with proton assignments in dmso-d_6 at 298 K. Figure S9: High-resolution ESI MS spectrum of (4). Figure S10: High-resolution ESI MS spectrum of (5). Inset, the calculated and the experimental (A) and the calculated (B) isotopic patterns of the cation. Figure S11: High-resolution ESI MS spectrum of (6). Figure S12: High-resolution ESI MS spectrum of (7). Inset, the calculated and the experimental (A) and the calculated (B) isotopic patterns of the cation. Figure S13: High-resolution ESI MS spectrum of (8). Inset, the calculated and the experimental (A) and the calculated (B) isotopic patterns of the cation. Figure S14: High-resolution ESI MS spectrum of (9). Inset, the calculated and the experimental (A) and the calculated (B) isotopic patterns of the cation. Figure S15: High-resolution ESI MS spectrum of (10). Figure S16: High-resolution ESI MS spectrum of (11). Figure S17. Normalized UV spectra of (1) and (2) in acetonitrile.

Author Contributions: Conceptualization, K.Y. and A.G. (Achilleas Garoufis); methodology, K.Y. and A.G. (Antonia Garypidou); validation, K.Y.; investigation, A.G. (Antonia Garypidou), A.G. (Andreas Gikas) and A.K.; writing—original draft preparation, A.G. (Antonia Garypidou), J.C.P. and A.G. (Achilleas Garoufis); writing—review and editing, A.G. (Antonia Garypidou), J.C.P. and A.G. (Achilleas Garoufis); supervision, A.G. (Achilleas Garoufis). All authors have read and agreed to the published version of the manuscript.

Funding: Antonia Garypidou and Konstantinos Ypsilantis were financially supported by the project "Center For Research, Quality Analysis Of Cultural Heritage Materials and Communication Of Science" (MIS 5047233) implemented under the Action "Reinforcement of the Research and Innovation Infrastructure", funded by the Operational Program "Competitiveness, Entrepreneurship and Innovation" (NSRF 2014-2020) and co-financed by Greece and the European Union (European Regional Development Fund).

Data Availability Statement: Not applicable.

Acknowledgments: We acknowledge the Unit of Environmental, Organic and Biochemical high-resolution analysis-ORBITRAP-LC-MS and the NMR Centre of the University of Ioannina for providing access to the facilities.

Conflicts of Interest: The authors declare no conflict of interest.

References

1. Champe, P.; Harvey, R. Amino Acids Amino Acids. *Lippincott's Illus. Rev. Biochem.* **2003**, *96*, 1–12. [CrossRef]
2. Hönig, M.; Sondermann, P.; Turner, N.J.; Carreira, E.M. Enantioselective Chemo- and Biocatalysis: Partners in Retrosynthesis. *Angew. Chem. Int. Ed.* **2017**, *56*, 8942–8973. [CrossRef]
3. Xue, Y.P.; Cao, C.H.; Zheng, Y.G. Enzymatic asymmetric synthesis of chiral amino acids. *Chem. Soc. Rev.* **2018**, *47*, 1516–1561. [CrossRef] [PubMed]
4. Patil, S.T.; Zhang, L.; Martenyi, F.; Lowe, S.L.; Jackson, K.A.; Andreev, B.V.; Avedisova, A.S.; Bardenstein, L.M.; Gurovich, I.Y.; Morozova, M.A.; et al. Activation of mGlu2/3 receptors as a new approach to treat schizophrenia: A randomized Phase 2 clinical trial. *Nat. Med.* **2007**, *13*, 1102–1107. [CrossRef] [PubMed]
5. Kindler, H.L.; Burris, H.A.; Sandler, A.B.; Oliff, I.A. A phase II multicenter study of L-alanosine, a potent inhibitor of adenine biosynthesis, in patients with MTAP-deficient cancer. *Investig. New Drugs* **2009**, *27*, 75–81. [CrossRef] [PubMed]

6. Blaskovich, M.A.T. Unusual Amino Acids in Medicinal Chemistry. *J. Med. Chem.* **2016**, *59*, 10807–10836. [CrossRef] [PubMed]
7. Axup, J.Y.; Bajjuri, K.M.; Ritland, M.; Hutchins, B.M.; Kim, C.H.; Kazane, S.A.; Halder, R.; Forsyth, J.S.; Santidrian, A.F.; Stafin, K.; et al. Synthesis of site-specific antibody-drug conjugates using unnatural amino acids. *Proc. Natl. Acad. Sci. USA* **2012**, *109*, 16101–16106. [CrossRef] [PubMed]
8. Yadav, V.N.; Comotti, A.; Sozzani, P.; Bracco, S.; Bonge-Hansen, T.; Hennum, M.; Görbitz, C.H. Microporous Molecular Materials from Dipeptides Containing Non-proteinogenic Residues. *Angew. Chem. Int. Ed.* **2015**, *54*, 15684–15688. [CrossRef]
9. Zerfas, B.L.; Coleman, R.A.; Salazar-Chaparro, A.F.; MacAtangay, N.J.; Trader, D.J. Fluorescent Probes with Unnatural Amino Acids to Monitor Proteasome Activity in Real-Time. *ACS Chem. Biol.* **2020**, *15*, 2588–2596. [CrossRef]
10. Gupta, A.; Garreffi, B.P.; Guo, M. Facile synthesis of a novel genetically encodable fluorescent α-amino acid emitting greenish blue light. *Chem. Commun.* **2020**, *56*, 12578–12581. [CrossRef]
11. Liu, Y.-J.; Liu, Y.-H.; Zhang, Z.-Z.; Yan, S.-Y.; Chen, K.; Shi, B.-F. Divergent and Stereoselective Synthesis of β-Silyl-α-Amino Acids through Palladium-Catalyzed Intermolecular Silylation of Unactivated Primary and Secondary C−H Bonds. *Angew. Chem.* **2016**, *128*, 14063–14066. [CrossRef]
12. Chen, K.; Hu, F.; Zhang, S.-Q.; Shi, B.-F. Pd(ii)-catalyzed alkylation of unactivated C(sp3)–H bonds: Efficient synthesis of optically active unnatural α-amino acids. *Chem. Sci.* **2013**, *4*, 3906–3911. [CrossRef]
13. He, G.; Wang, B.; Nack, W.A.; Chen, G. Syntheses and Transformations of α-Amino Acids via Palladium-Catalyzed Auxiliary-Directed sp3 C-H Functionalization. *Acc. Chem. Res.* **2016**, *49*, 635–645. [CrossRef]
14. Sengupta, S.; Mehta, G. Late stage modification of peptides via C[sbnd]H activation reactions. *Tetrahedron Lett.* **2017**, *58*, 1357–1372. [CrossRef]
15. Manallack, D.T.; Prankerd, R.J.; Nassta, G.C.; Ursu, O.; Oprea, T.I.; Chalmers, D.K. A Chemogenomic Analysis of Ionization Constants-Implications for Drug Discovery. *ChemMedChem* **2013**, *8*, 242–255. [CrossRef] [PubMed]
16. Kumar, H.; Kaur, K. Interaction of antibacterial drug ampicillin with glycine and its dipeptides analyzed by volumetric and acoustic methods at different temperatures. *Thermochim. Acta* **2013**, *551*, 40–45. [CrossRef]
17. Feng, H.; Ding, J.; Zhu, D.; Liu, X.; Xu, X.; Zhang, Y.; Zang, S.; Wang, D.C.; Liu, W. Structural and mechanistic insights into NDM-1 catalyzed hydrolysis of cephalosporins. *J. Am. Chem. Soc.* **2014**, *136*, 14694–14697. [CrossRef]
18. Yang, M.; Jiang, X.; Shi, Z.J. Direct amidation of the phenylalanine moiety in short peptides via Pd-catalyzed C-H activation/C-N formation. *Org. Chem. Front.* **2015**, *2*, 51–54. [CrossRef]
19. Tao, Q.; Li, Y.N.; Tang, W.J.; Liu, P.Y.; Yu, F.; He, Y.P. Di-ortho-C[sbnd]H arylation of phenylalanine: A bimetallic interaction between Pd(IV)-Ag(I). *Tetrahedron Lett.* **2021**, *74*, 153158. [CrossRef]
20. Schubert, U.S.; Winter, A.; Newkome, G.R. *Terpyridine-Based Materials: For Catalytic, Optoelectronic and Life Science Applications*; Wiley-VCH Verlag GmbH & Co., KGaA: Weinheim, Germany, 2012.
21. Fan, Y.; Zhu, Y.M.; Dai, F.R.; Zhang, L.Y.; Chen, Z.N. Photophysical and anion sensing properties of platinum(ii) terpyridyl complexes with phenolic ethynyl ligands. *J. Chem. Soc. Dalt. Trans.* **2006**, 3885–3892. [CrossRef]
22. Ma, Z.; Lu, W.; Liang, B.; Pombeiro, A.J.L. Synthesis, characterization, photoluminescent and thermal properties of zinc(ii) 4′-phenyl-terpyridine compounds. *New J. Chem.* **2013**, *37*, 1529–1537. [CrossRef]
23. Ma, Z.; Wang, Q.; Alegria, E.C.B.A.; Da Silva, M.F.C.G.; Martins, L.M.D.R.S.; Telo, J.P.; Correia, I.; Pombeiro, A.J.L. Synthesis and structure of copper complexes of a N_6O_4 macrocyclic ligand and catalytic application in alcohol oxidation. *Catalysts* **2019**, *9*, 424. [CrossRef]
24. Shikhova, E.; Danilov, E.O.; Kinayyigit, S.; Pomestchenko, I.E.; Tregubov, A.D.; Camerel, F.; Retailleau, P.; Ziessel, R.; Castellano, F.N. Excited-state absorption properties of platinum(II) terpyridyl acetylides. *Inorg. Chem.* **2007**, *46*, 3038–3048. [CrossRef] [PubMed]
25. Ma, Z.; Cao, Y.; Li, Q.; Guedes da Silva, M.F.C.; Fraústo da Silva, J.J.R.; Pombeiro, A.J.L. Synthesis, characterization, solid-state photo-luminescence and anti-tumor activity of zinc(II) 4′-phenyl-terpyridine compounds. *J. Inorg. Biochem.* **2010**, *104*, 704–711. [CrossRef]
26. Mughal, E.U.; Mirzaei, M.; Sadiq, A.; Fatima, S.; Naseem, A.; Naeem, N.; Fatima, N.; Kausar, S.; Altaf, A.A.; Zafar, M.N.; et al. Terpyridine-metal complexes: Effects of different substituents on their physico-chemical properties and density functional theory studies: Properties of terpyridine base complexes. *R. Soc. Open Sci.* **2020**, *7*, 201208. [CrossRef] [PubMed]
27. Ryan, R.T.; Stevens, K.C.; Calabro, R.; Parkin, S.; Mahmoud, J.; Kim, D.Y.; Heidary, D.K.; Glazer, E.C.; Selegue, J.P. Bis-tridentate N-Heterocyclic Carbene Ru(II) Complexes are Promising New Agents for Photodynamic Therapy. *Inorg. Chem.* **2020**, *59*, 8882–8892. [CrossRef] [PubMed]
28. Jakubikova, E.; Chen, W.; Dattelbaum, D.M.; Rein, F.N.; Rocha, R.C.; Martin, R.L.; Batista, E.R. Electronic structure and spectroscopy of $[Ru(tpy)_2]^{2+}$, $[Ru(tpy)(bpy)(H_2O)]^{2+}$, and $[Ru(tpy)(bpy)(Cl)]^{+}$. *Inorg. Chem.* **2009**, *48*, 10720–10725. [CrossRef] [PubMed]
29. Paul, S.; Kundu, P.; Kondaiah, P.; Chakravarty, A.R. BODIPY-Ruthenium(II) Bis-Terpyridine Complexes for Cellular Imaging and Type-I/-II Photodynamic Therapy. *Inorg. Chem.* **2021**, *60*, 16178–16193. [CrossRef] [PubMed]
30. Hofmeier, H.; Schubert, U.S. Recent developments in the supramolecular chemistry of terpyridine–metal complexes. *Chem. Soc. Rev.* **2004**, *33*, 373–399. [CrossRef] [PubMed]
31. Puntoriero, F.; Campagna, S.; Stadler, A.; Lehn, J. Luminescence properties and redox behavior of Ru(II) molecular racks. *Coord. Chem. Rev.* **2008**, *252*, 2480–2492. [CrossRef]

32. Liu, P.; Shi, G.; Chen, X. Terpyridine-Containing π-Conjugated Polymers for Light-Emitting and Photovoltaic Materials. *Front. Chem.* **2020**, *8*, 592055. [CrossRef] [PubMed]
33. Sauvage, J.P.; Collin, J.P.; Chambron, J.C.; Guillerez, S.; Coudret, C.; Balzani, V.; Barigelletti, F.; De Cola, L.; Flamigni, L. Ruthenium(II) and Osmium(II) Bis(terpyridine) Complexes in Covalently-Linked Multicomponent Systems: Synthesis, Electrochemical Behavior, Absorption Spectra, and Photochemical and Photophysical Properties. *Chem. Rev.* **1994**, *94*, 993–1019. [CrossRef]
34. Ziessel, R. Making New Supermolecules for the Next Century: Multipurpose Reagents from Ethynyl-Grafted Oligopyridines. *Synthesis* **1999**, *1999*, 1839–1865. [CrossRef]
35. Breivogel, A.; Hempel, K.; Heinze, K. Dinuclear bis(terpyridine)ruthenium(II) complexes by amide coupling of ruthenium amino acids: Synthesis and properties. *Inorg. Chim. Acta* **2011**, *374*, 152–162. [CrossRef]
36. Ypsilantis, K.; Plakatouras, J.C.; Manos, M.J.; Kourtellaris, A.; Markopoulos, G.; Kolettas, E.; Garoufis, A. Stepwise synthesis, characterization, DNA binding properties and cytotoxicity of diruthenium oligopyridine compounds conjugated with peptides. *Dalt. Trans.* **2018**, *47*, 3549–3567. [CrossRef]
37. Akasaka, T.; Inoue, H.; Kuwabara, M.; Mutai, T.; Otsuki, J.; Araki, K. Synthesis and properties of an efficient and switchable photosensitizing unit, [Ru(4,4′-diphenyl-2,2′-bipyridine)$_2$(7-amino-dipyrido[3,2-a:2′,3′-c]phenazine)]$^{2+}$, for a photo-induced energy transfer systemElectronic supplementary information (ESI) available. *Dalt. Trans.* **2003**, 815–821. [CrossRef]
38. Wang, H.; Ji, X.; Li, Z.; Zhu, C.N.; Yang, X.; Li, T.; Wu, Z.L.; Huang, F. Preparation of a white-light-emitting fluorescent supramolecular polymer gel with a single chromophore and use of the gel to fabricate a protected quick response code. *Mater. Chem. Front.* **2017**, *1*, 167–171. [CrossRef]
39. Smith, C.B.; Raston, C.L.; Sobolev, A.N. Poly(ethyleneglycol)(PEG): A versatile reaction medium in gaining access to 4′-(pyridyl)-terpyridines. *Green Chem.* **2005**, *7*, 650–654. [CrossRef]
40. Bhaumik, C.; Das, S.; Saha, D.; Dutta, S.; Baitalik, S. Synthesis, Characterization, Photophysical, and Anion-Binding Studies of Luminescent Heteroleptic Bis-Tridentate Ruthenium(II) Complexes Based on 2,6-Bis(Benzimidazole-2-yl)Pyridine and 4′-Substituted 2,2′:6′,2′′ Terpyridine Derivatives. *Inorg. Chem.* **2010**, *49*, 5049–5062. [CrossRef]
41. Spahni, W.; Calzagerri, G. Synthese vonpara-substituierten phenyl-terpyridin liganden. *Helv. Chim. Acta* **1984**, *67*, 450–454. [CrossRef]
42. Laurent, F.; Plantalech, E.; Donnadieu, B.; Jiménez, A.; Hernández, F.; Martínez-Ripoll, M.; Biner, M.; Llobet, A. Synthesis, structure and redox properties of ruthenium complexes containing the tpm facial and the trpy meridional tridentate ligands. *Polyhedron* **1999**, *18*, 3321–3331. [CrossRef]
43. Elsbernd, H.; Beattie, J.K. The NMR spectra of terpyridine and the bis-terpyridine complexes of cobalt(III) and iron(II). *J. Inorg. Nucl. Chem.* **1972**, *34*, 771–774. [CrossRef]
44. Pazderski, L.; Pawlak, T.; Sitkowski, J.; Kozerski, L.; Szlyk, E. 1H, 13C, 15N NMR coordination shifts in Fe(II), Ru(II) and Os(II) cationic complexes with 2,2′:6′,2′′-terpyridine. *Magn. Reson. Chem.* **2011**, *49*, 237–241. [CrossRef] [PubMed]
45. Stone, M.L.; Crosby, G.A. Charge-transfer luminescence from ruthenium(II) complexes containing tridentate ligands. *Chem. Phys. Lett.* **1981**, *79*, 169–173. [CrossRef]
46. Jain, N.; Mary, A.; Manjunath, V.; Sakla, R.; Devan, R.S.; Jose, D.A.; Naziruddin, A.R. Ruthenium (II) Complexes Bearing Heteroleptic Terpyridine Ligands: Synthesis, Photophysics and Solar Energy Conversion. *Eur. J. Inorg. Chem.* **2021**, *2021*, 5014–5023. [CrossRef]
47. Maestri, M.; Armaroli, N.; Balzani, V.; Constable, E.C.; Thompson, A.M.W.C. Complexes of the Ruthenium(II)-2,2′:6′,2′′ -Terpyridine Family. Effect of Electron-Accepting and -Donating Substituents on the Photophysical and Electrochemical Properties. *Inorg. Chem.* **1995**, *34*, 2759–2767. [CrossRef]
48. Zhang, R.; Yu, X.; Ye, Z.; Wang, G.; Zhang, W.; Yuan, J. Turn-on Luminescent Probe for Cysteine/Homocysteine Based on a Ruthenium(II) Complex. *Inorg. Chem.* **2010**, *49*, 7898–7903. [CrossRef]
49. Juris, A.; Balzani, V.; Barigelletti, F.; Campagna, S.; Belser, P.; von Zelewsky, A. Ru(II) polypyridine complexes: Photophysics, photochemistry, eletrochemistry, and chemiluminescence. *Coord. Chem. Rev.* **1988**, *84*, 85–277. [CrossRef]
50. Meyer, T.J. Photochemistry of metal coordination complexes: Metal to ligand charge transfer excited states. *Pure Appl. Chem.* **1986**, *58*, 1193–1206. [CrossRef]